THE ASTROPHYSICAL JOURNAL, 456:L67–L70, 1996 January 1

THE NEAR-INFRARED CORONAL SPECTRUM

J. R. KUHN
National Solar Observatory/Sacramento Peak, National Optical Astronomy Observatories,[1]
P.O. Box 62, Sunspot, NM 88349; and
Michigan State University, Department of Physics and Astronomy

M. J. PENN
National Solar Observatory/Sacramento Peak, National Optical Astronomy Observatories,[1]
P.O. Box 62, Sunspot, NM 88349

AND

I. MANN
Max-Planck-Institute für Aeronomie, Postfach 20, D-37189 Katlenburg-Lindau, Germany
Received 1995 September 18; accepted 1995 October 24

ABSTRACT

Sensitive measurements of the near-infrared coronal spectrum were obtained from the 1994 total solar eclipse. A new [S IX] emission line at 1.25249 ± 0.00003 μm has been detected, and a bright, potentially important diagnostic, [Si X] line at 1.43 μm has been confirmed. Upper limits on the intensity of several other predicted IR emission lines have been established. Also, diffuse He I emission, perhaps geocoronal, has been observed with a significant heliocentric redshift.

Subject headings: line: identification — Sun: corona — Sun: infrared

The outstanding problem of how magnetic fields define the structure and temperature of the solar corona exists largely because there are no general techniques for measuring these fields. Methods using background radio sources or gyroresonance measurements can provide limited information (cf. Bird & Eidenhofer 1991 or Lee, Hurford, & Gary 1993). Near-infrared optical Zeeman splitting observations are promising (Kuhn 1995) but have not yet been proved. It may be possible to measure the weak magnetic fields that dominate the corona if bright coronal infrared emission lines can be found, since magnetic sensitivity and the optical Zeeman splitting increase with increasing wavelength.

Surprisingly, we know relatively little about the IR coronal spectrum. The most recent measurements are aircraft Fourier transform spectroscope (FTS) observations dating from the early 1970s (Olsen, Anderson, & Stewart 1971). Unfortunately, attempts to confirm these measurements using a coronagraph and modern IR array detectors (Penn & Kuhn 1994) suggest that the earlier detections may be "optimistic." We report here on what we believe to be the first sensitive measurement of the near-infrared coronal spectrum, obtained during the 1994 total eclipse.

The well-known eclipse disadvantages, namely short duration and complex logistics, are amply compensated by the decrease in sky background. Our practical emission-line detection threshold improved by ~2 orders of magnitude from typical coronagraph observations (cf. Penn 1995). Background-limited IR array detectors make the problem of obtaining eclipse spectra straightforward. For this experiment we designed and built a compact Newtonian telescope/Ebert-Fastie Spectrograph/NICMOS III IR camera system. This will be described in greater detail elsewhere. In short, a 15 cm Newtonian telescope fed light to an f/7 Ebert-Fastie spectrograph and a 256 × 256 pixel HgCdTe 1–2.5 μm camera. The system uses reflecting planar and spherical optics except for a low-power cylindrical lens that was used to correct the astigmatism of the spectrograph collimator. The slit width was 80 μm (corresponding to 2 pixels), and the detector/slit had a projected length on the sky of 1820″ (1.9 $R_\odot$). The grating (at ambient temperature) was used in first order and yielded a dispersion of ~0.09 nm pixel^{-1} over the 1–1.5 μm spectral range of these observations. Our measured FWHM of unresolved spectral features was ~3 pixels or 0.3 nm. An equatorial mount kept the 35 kg telescope/spectrograph/liquid nitrogen Dewar and camera tracking the Sun. A PC controlled the grating rotation and a digital signal processor (DSP) that interfaced to the IR array camera. The telescope pointing was controlled with a clock drive and manual offset adjustments. A commercial camcorder was mounted along the telescope tube to record the telescope pointing and the eclipse in the visible.

Our location near the village of Putre in the northern Chilean Andes was at an altitude of ~3700 m (12,000 feet). The site was dry, and during the 12 days we were there it was mostly cloudless—except for the day of the eclipse. Before and during totality there was cirrus in the general direction of the Sun. As we note below, the cirrus was apparent in our spectrophotometry.

Most of the duration of totality (120 s of the 178 s) was used to obtain 45 spectral frames. The primary slit position is shown on the HAO (Lucinski et al. 1994) white-light radial-gradient filter eclipse image in Figure 1 (Plate L9). A pair of 1 s exposures at each grating angle were obtained with the IR array, were co-added with the DSP, and were stored on the PC hard disk. The grating angle was changed a small amount to move the coronal spectrum across the array; each wavelength was observed at least twice, as the spectrum was scanned less than half of the field of view of the array. After this spectral scan was complete, two long integrations (10 1 s exposures co-added) at the grating angle of the 1.28 μm 5–3 H I Paschen line were made, one at the primary slit position, and the

[1] Operated by the Association of Universities for Research in Astronomy, Inc. (AURA), under cooperative agreement with the National Science Foundation.

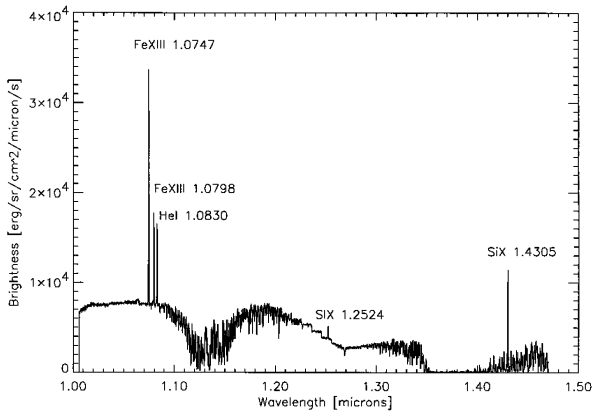

FIG. 2a

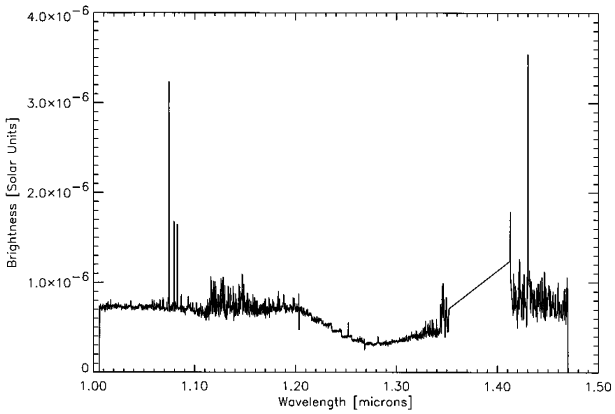

FIG. 2b

FIG. 2.—The mean IR coronal spectrum from 43″ near the limb. (*a*) The intensity calibration assumes an apparent solar disk brightness of 1.2×10^{10} ergs s^{-1} cm^{-2} sr^{-1} μm^{-1}. (*b*) The coronal spectrum has been normalized by the disk brightness. Photospheric and variable atmospheric absorption lines were not corrected from the disk spectrum.

second south of the solar south pole. Dark current measurements were also taken during totality. The remaining calibration data (incandescent lamp flat-field images and calibration solar spectra) were taken after the third contact, with the same grating scan sequence used during totality.

The calibration, or flat-fielding, of the spectra was more complicated than most array-type observations. Since flat-field images must be recorded after the eclipse and after the grating has moved, the flat fields obtained with the lamp have a slightly different fringe pattern than the eclipse data. To correct this problem, we devised a two-dimensional generalization of the one-dimensional Hilbert transform (Bracewell 1965, p. 241), which we applied to the lamp data at each grating position. The resulting phase function could then be finely adjusted to account for the fringe pattern in the eclipse data. These details of the detector calibration model will also be described elsewhere. The detector saturates at ~9000 "data numbers" and has a total noise per read of ~20 DN. The residual flat-fielding noise generally had an amplitude of less than 2%. Spectral intensities were calibrated against the solar spectrum obtained with the (nearly) full-aperture neutral density filter. The spectral response of the neutral density filter was measured in the laboratory between 0.8 and 1.5 μm with a monochromator and found to be a smooth function of wavelength.

The average infrared coronal spectrum from 43″ (6 pixels) near the lunar limb is displayed in Figure 2*a*. The wavelength scale for each of the 45 spectra was obtained by cross-correlating the data with the NSO/Kitt Peak IR atlas (Livingston & Wallace 1991), and the intensity calibration was obtained from observations of the disk after the third contact. Overlapping spectral regions were averaged to obtain the continuous spectrum of Figure 2*a*. Note that most of the structure in the spectrum results from atmospheric absorption. To correct for absorption, Figure 2*b* shows the coronal spectrum normalized by the disk brightness. This normalization produces deceptive local peaks at wavelengths where the disk spectrum has strong Fraunhofer lines or where atmospheric extinction is large and variable. Note that the continuum brightness is apparently independent of wavelength, except for the decrease near 1.2–1.4 μm. This intensity drop occurs as cirrus intervene during the eclipse. The cloud extinction decreases again toward the third contact, i.e., longer wavelengths in the spectral sequence.

Despite the extinction and scattered light due to the variable cirrus, our detection threshold for coronal emission lines is significantly lower than previous measurements. Between 1.08 and 1.47 μm and at wavelengths outside of strong atmospheric absorption, these measurements will detect emission brighter than 3×10^{-8} of the disk brightness. The strongest lines in Figure 2 (at 1.0747 and 1.0798 μm) are from [Fe XIII] (cf. Penn & Kuhn 1994). Emission from cool neutral He in the prominence is also visible at 1.083 μm. [Si X] emission at 1.4308 μm is confirmed by these data to have a brightness comparable to the 1.0747 μm [Fe XIII] emission line. It should be sensitive to magnetic fields ~40% smaller than [Fe XIII] and may prove to be useful for coronal magnetometry.

We see a new line at 1.25249 ± 0.00003 μm. Based on the wavelength predictions of Kaufmann & Sugar (1986), [S IX] is responsible for this emission. The predicted wavelength agrees with our observations to within the wavelength uncertainties. The excitation potential (379 eV) and the lower abundance of sulfur are also consistent with the weaker emission. While neither the observed line strength nor wavelength of the new line detection are consistent with the earlier aircraft solar eclipse experiment (Olsen et al. 1971), the [S IX] line wavelength does agree with the lower spectral resolution observations of Nova Cygni 1992 (Woodward et al. 1995). Limits on other predicted lines (Kaufmann & Sugar 1986; Kastner 1995; Chang & Deming 1995) in the 1–1.5 μm range and our detections are summarized in Table 1.

Our spectroscopic measurements of [Fe XIII] lines extend to nearly $2\,R_\odot$ beyond the limb. It is also interesting that the 1.083 μm He I line is visible at large angles from the limb. Scattered light that results from cirrus and the prominence extending beyond the lunar limb is an important concern. Fortunately, the integration period of our last spectrum (covering the 1.28 μm H I line) ended after the third contact and provided a quantitative measure of cloud-scattered chromospheric light. The H I Paschen line was seen in emission even though the spectrograph field of view did not include the exposed chromosphere. The radial variation in intensity of this emission implies a scattering function that falls exponentially with a scale length of 920″ (130 pixels). Figure 3*a* shows the line

TABLE 1

POSSIBLE CORONAL EMISSION LINES AND OBSERVED DETECTION LIMITS OR DETECTIONS

λ (μm) (1)	Reference (2)	Species (3)	Upper Limit (or Detection) (4)
1.01064	KS	Cr VIII	150
1.01300	KS	Cu XV	150
1.0159	KS	Ar XIII	80
1.0264	KS	S XIII	80
1.0308	KS	P XI	150
1.0311	KS	V XI	80
1.0436	KS	Cu XVIII	80
1.0672	KS	Cl XII	80
1.07469	KS	Fe XIII	(7800)
1.07979	KS	Fe XIII	(3000)
1.08780	KS	Cr XIII	80
1.1110	KS	K XVI	150
1.1478	KS	Co XIII	150
1.202	K	Fe XIV	80
1.2060	KS	Ge XVII	80
1.2150	KS	Ni XVII	80
1.2520	KS	S IX	(330)
1.2783	KS	Cr IX	80
1.2815	KS	Ni XIV	80
1.2817	KS	Mn XII	80
1.3038	KS	V VII	80
1.3070	KS	Ca XIV	80
1.3254	KS	Ti X	80
1.3450	KS	K XIII	30
1.3745	KS	P VII	12
1.3774	KS	Cl XII	30
1.3885	KS	Mn XII	12
1.3904	KS	Ar XV	12
1.3924	KS	S XI	12
1.3951	KS	P XII	12
1.3963	KS	V XII	12
1.4200	KS	Mn XVII	30
1.4300	KS	Co XVI	3300
1.4301	KS	Si X	(3300)

NOTES.—Col. (1) identifies the theoretical wavelength in microns. Col. (2) shows the reference: KS, Kaufman & Sugar 1986; K, Kastner 1995. Col. (3) gives the ionization state. Col. (4) gives our estimated 2σ upper limit to the line emission (or detection) in 10^{-3} ergs s^{-1} cm^{-2} sr^{-1}, from 43″ averaged near the limb.

intensity variation of the observed He I emission and the nearby continuum intensity change along the slit. For comparison, Figure 3*b* shows the corresponding variation of the [Fe XIII] 1.0747 μm line and nearby continuum. Evidently the

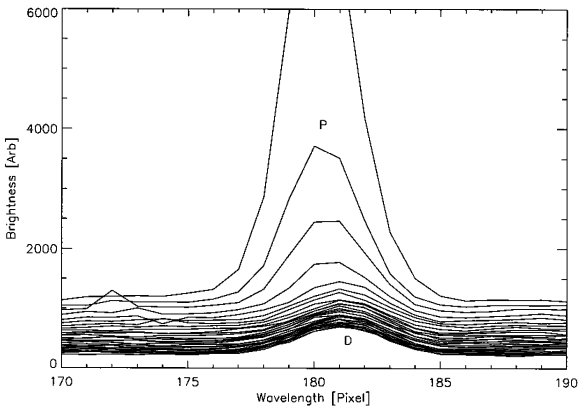

FIG. 4.—Overplotted spectral line profiles of the He I emission from 30 pixels (213″) near the limb. The symbol "P" indicates the line-center position of the prominence He I emission, and "D" indicates the shifted line-center position of the diffuse emission component.

spatial variation of the He I emission is unrelated to scattered light from localized sources in the corona or to any diffuse coronal emission with an electron density dependence comparable to the Fe XIII emission mechanism.

Further evidence that the diffuse He I emission is *not* scattered light is apparent from the line profiles. Figure 4 shows overplotted spectra from pixel columns near the lunar limb out to 30 pixels beyond the limb. The bright emission near the limb results from the prominence. Away from the limb, extending at least 1.8 $R_\odot$, there is a component that is redshifted by $\sim 25 \pm 5$ km s^{-1}. Note that although the He I triplet is unresolved by our measurements, it is unlikely that intensity variations between the components could cause the apparent mean lineshift.

While the velocity shift between the diffuse and near-solar components is well established, our absolute wavelength scale is not accurate enough to fix the heliocentric velocity of the He I emission components to better than ~20 km s^{-1}. The two data frames that include the He I lines show the same results. Also, the [Fe XIII] lines have a similar intensity near the limb but do not show the line profile shifts observed in He I.

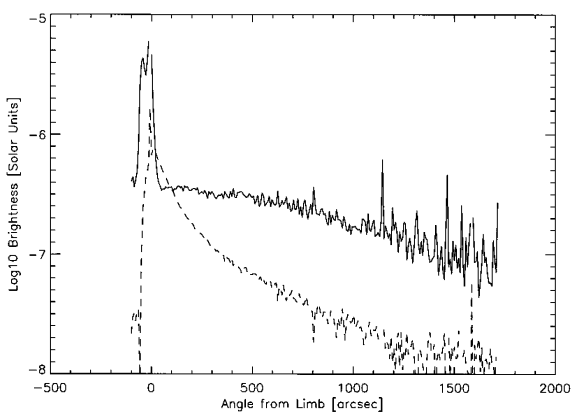

FIG. 3*a*

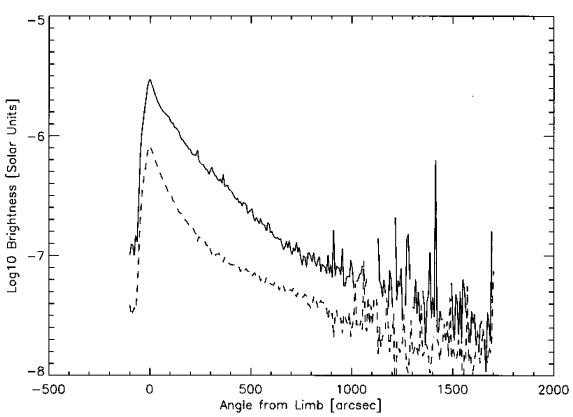

FIG. 3*b*

FIG. 3.—(*a*) The derived He I 1.083 μm line amplitude variation along the slit (*solid line*), and the nearby continuum variation (*dashed line*). (*b*) The [Fe XIII] 1.0747 μm line amplitude variation (*solid line*), and nearby continuum (*dashed line*).

We are confident that the diffuse He I component does not result from scattered light from prominence emission but we cannot clearly identify its source. Interstellar neutral He gas has been optically detected in the solar system (cf. Holzer 1977) and by in situ measurements (Witte et al. 1993) with a heliocentric velocity of 26 km s^{-1}. Unfortunately, the direction of this interstellar wind is not consistent with the redshift we observe for the diffuse component. A more likely origin may be diffuse emission from the local geocoronal He "atmosphere." A highly variable terrestrial He atmosphere (which changes with the solar EUV brightness) has been observed in the light of He I 1.083 μm (Christensen, Patterson, & Tinsley 1968). The surface brightness we see is ~2–3 orders of magnitude brighter than these geocoronal measurements 8° from the Sun. No other data are available for these small angles, but the earlier measurements do show a rapidly rising He I surface brightness toward the Sun. Thus, even though a quantitative comparison with the geophysical observations is not possible, it is possible that the diffuse He emission we see toward the Sun originates from the geocorona.

Roy Coulter, Jim Mason, Robert McGraw, and Larry Wilkins were an important part of the eclipse expedition that made these measurements possible. Jim Mason assisted with the spectrograph construction, and Serge Koutchmy loaned us an infrared grating. Bob MacQueen also participated in the early stages of this experiment. Logistical support within Chile was generously provided by Hernan Bustos and Erie Vasquez. This research was supported by the NSF through the Solar Terrestrial and Atmospheric Science Divisions.

REFERENCES

Bird, M. K., & Edenhofer, P. 1991, in Physics and Chemistry in Space, Physics of the Inner Heliosphere, ed. R. Schwenn & E. Marsch (Heidelberg: Springer), 13
Bracewell, R. 1965, The Fourier Transform and Its Applications (New York: McGraw-Hill)
Chang, E. S., & Deming, D. 1995, in Infrared Tools for Solar Astrophysics: What's Next? ed. J. R. Kuhn & M. J. Penn (Singapore: World Scientific), 47
Christensen, A. B., Patterson, J. N. L., & Tinsley, B. A. 1968, J. Geophys. Res., 76, 1764
Holzer, T. E. 1977, Rev. Geophys. Space Sci., 15, 467
Kastner, S. 1995, in Infrared Tools for Solar Astrophysics: What's Next? ed. J. R. Kuhn & M. J. Penn (Singapore: World Scientific), 55
Kaufman, V., & Sugar, J. 1986, J. Phys. Chem. Ref. Data, 15, 321
Kuhn, J. R. 1995, in Infrared Tools for Solar Astrophysics: What's Next? ed. J. R. Kuhn & M. J. Penn (Singapore: World Scientific), 89
Lee, J. W., Hurford, G. J., & Gary, D. E. 1993, Sol. Phys., 144, 349
Livingston, W., & Wallace, L. 1991, National Solar Obs. Tech. Rep., No. 91-001
Lucinski, A., et al. 1994, private communication
Olsen, K. H., Anderson, C. R., & Stewart, J. N. 1971, Sol. Phys., 21, 360
Penn, M. J. 1995, in Infrared Tools for Solar Astrophysics: What's Next? ed. J. R. Kuhn & M. J. Penn (Singapore: World Scientific), 69
Penn, M. J., & Kuhn, J. R. 1994, ApJ, 434, 807
Witte, M., Rosenbauer, H., Banaszkiewicz, M., & Fahr, H. 1993, Adv. Space Res., 13(6), 121
Woodward, C. E., Greenhouse, M. A., Gehrz, R. D., Pendleton, Y. J., Joyce, R. R., Van Buren, D., Fischer, J., Jennerjohn, N. J., & Kaminski, C. D. 1995, ApJ, 438, 921

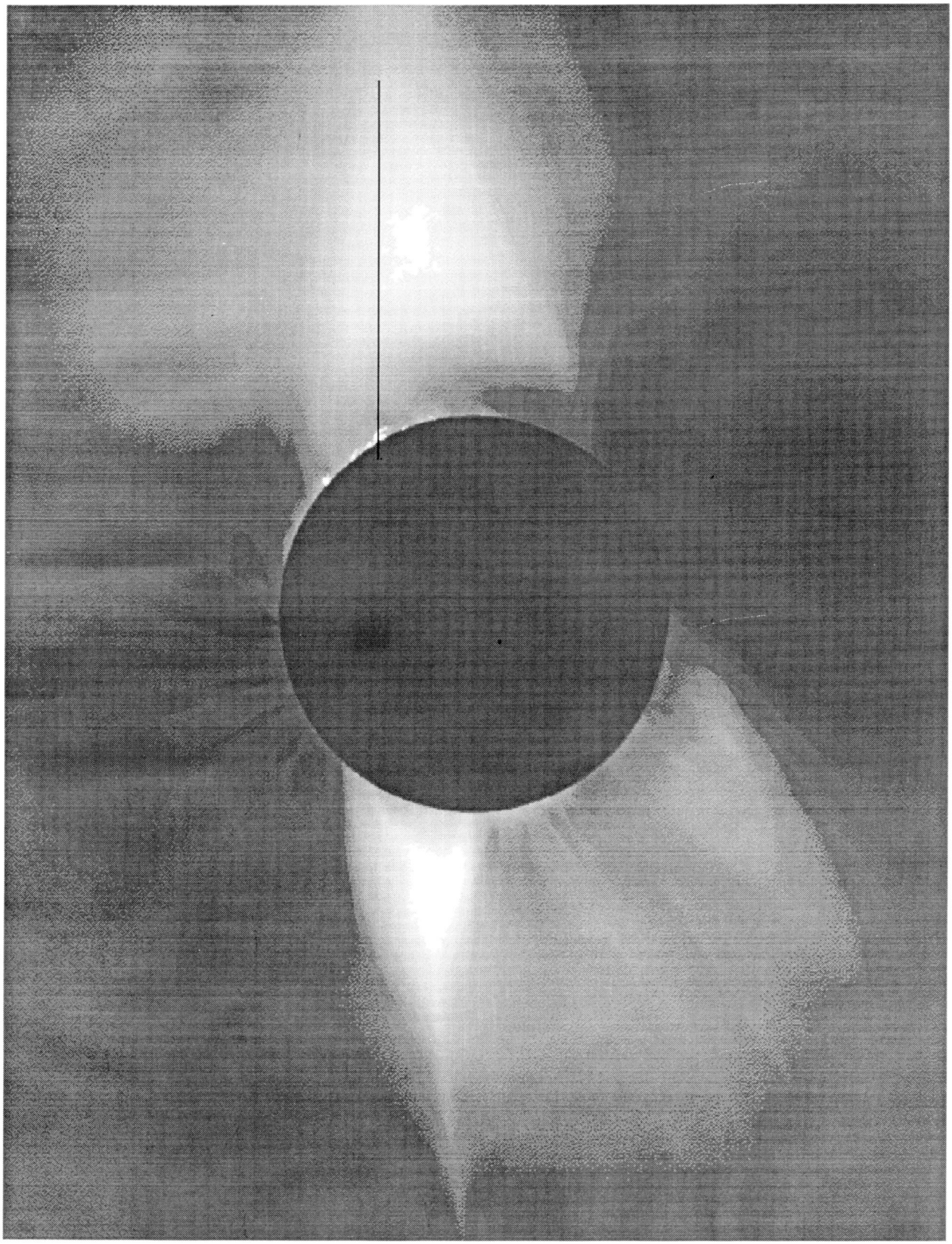

FIG. 1.—The primary slit position is shown here superposed over the HAO white-light 1995 eclipse image. North is up, and the slit covers a prominence on the east limb.

KUHN, PENN, & MANN (see 456, L67)